Original scientific paper

Informacije MIDEM
Journal of Microelectronics,
Electronic Components and Materials
Vol. 44, No. 1 (2014), 40 – 52

Supercapacitor Energy Storage System for Improving the Power flow in Photovoltaic Plants

Miguel Ángel Guerrero-Martínez, Enrique Romero-Cadaval, Víctor Miñambres-Marcos and María Isabel Milanés-Montero

Power Electrical and Electronics Systems (PE&ES), University of Extremadura, Spain

Abstract: Recently new elements have been added to the distribution grids which have changed the way the grids operate; this change in performance can affect the safety and reliability of management of the distribution grids. The disadvantages due to the changes in energy production justify the search for power injection systems capable of damping these changes. It is necessary that these power injection systems change their passive performance in the grid, becoming active elements that are integrated into the management of it, obtaining not only no negative effects on the grid, but also enhancing its reliability and operating possibilities. One of the major drawbacks of renewable energy generation is the change in energy production. This justifies the search for power injection systems capable of absorbing such fluctuations. In this paper, we present an injection system capable of integrating a photovoltaic generation system as a quasi-manageable generation system, incorporating the energy storage to moderate fluctuations in the energy generated, using a set of supercapacitors. With these functions, the inverters will become active parts of the grid, developing the concept of smart grid, which is generally accepted as the evolution of the current grid towards the one that will exist in the future. The system is composed of a voltage source inverter that injects the power into the grid, while a bidirectional direct current converter regulates the charge of the supercapacitor.

Keywords: Photovoltaic Plants, Power Injection Systems, Solar Energy, Energy Storage System, Supercapacitor

Sistem hranjenja energije s super kondenzatorjem za izboljšanje pretoka energije v fotonapetostnih sistemih

Izvleček: Nedavno se je v električno omrežje dodalo nove elemente, ki vplivajo na učinkovitost varnost in zanesljivost omrežij. Ta slabost potrjuje iskanje sistemov, ki zmanjšujejo njihov vpliv na omrežja. Pomembno je, da ti pasivni sistemi postanejo aktivni in ne zmanjšujejo le negativnih vplivov temveč celo izboljšujejo omrežja. Ena izmed glavni slabosti obnovljivih virov energije je njihova spremenljivost proizvodnje. V članku je predstavljen sistem, ki je sposoben omiliti vplive fluktuacij obnovljivih virov energije s vključitvijo hranilnikov energije v obliki super kondenzatorjev.

Ključne besede: fotonapetostni sistemi, napajalni sitemi, sončna energija, hranilniki energije, super kondenzatorji

* *Corresponding Author's e-mail: mguerrero@peandes.net*

1 Introduction

During the last few years, due to the regulatory framework for renewable energy, the number of Photovoltaic Generation Systems (PVGS) connected to the grid is experiencing a dramatic increase.

One of the main disadvantages of photovoltaic generation is that it limits the power granted to the evacuation points, due to its consideration as an unmanageable power source, which prevents ensuring the dynamic stability of the grid.

So that the PVGS do not affect the behavior of the grid, they must not only meet the supply to the grid specifications about quality and reliability, but must also ensure their successful integration, controlling the power generation curve. The generation curve is

highly dependent on climatic conditions [1] making its prediction and integration difficult in a planned system of generation [2], [3]. At present, these problems will not seriously affect the operation of the grid, but could become important in a near future with the present forecasting for integrating unmanaged renewable energy sources.

One possible solution to this problem could be that the photovoltaic generation systems acted as "quasi-manageable", generating energy at constant power during periods of time, whose value will be communicated previously to the manager responsible of the grid to which it connects. In order to function in this way, an energy storage system is needed, whose design, sizing and composition is determined in this article.

With this function, inverters will become active parts of the grid, able to assist in the management, planning and operation of these grids, achieving one of the main objectives in research and development of the European technological platform of smart grids.

PVGSs generated power fluctuations produce, in many cases, inversions of the net power flows in the head of the lines where they are connected. Fig. 1 shows the power measured in a line of the substation (Fig. 2) belonging to a rural meshed distribution grids, where there is a 1 MWp PVGS and less than 200 conventional customers (that sum up about 5 MW of contracted power capacity). Fig. 2 has been obtained using a Power Quality Meter (Topas 1000), and one can observe that there are not only rapid fluctuations of power, but also inversions of the net power flow in the line.

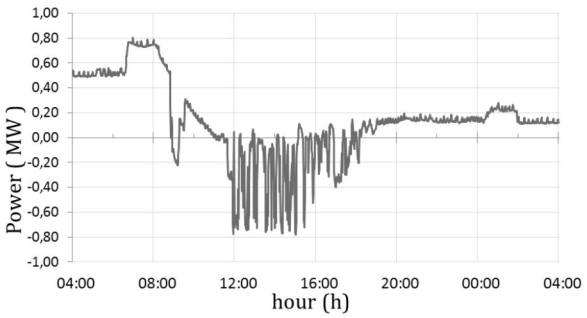

Figure 1: Power exiting the substation versus the time of the day.

Conventional power injection systems (PIS) of PVGSs are not designed to avoid these fluctuations. These systems usually consist of a DC-DC converter, which adapts the voltage of the photovoltaic system and tracks the maximum power point (MPPT), and of an inverter that converts DC-voltage into alternating voltage, controlling the current that is injected into the grid and seeking the power factor to be one [1].

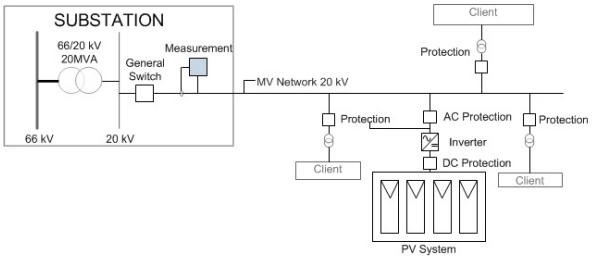

Figure 2: Installation diagram for the analyzer in the Substation.

Some effects of power fluctuation into the grid have been observed, for example, sudden drops in output power of 25 % in less than 3 minutes, especially in suburban and rural grids, and significant changes in the expected energy flow causing operational problems [3], [4].

In this paper, to give the PIS capacity to mitigate power fluctuations, it is necessary to include in its structure a storage element capable of absorbing energy.

This paper describes the principal energy storage technologies and discusses the possibility of using a supercapacitor energy storage system and shows how to integrate it. A supercapacitor energy storage system has been selected because it is easy to implement in present PIS structures and stores the energy in its original electrical form. Therefore, this technology is incipient and it is expected that it will have a great development in a near future.

2 Energy storage systems

To ensure continuity of supply in an environment in which a significant percentage of generation comes from renewable energy sources, Energy Storage Systems (ESS) are needed. This is one of the ideas behind the establishment of micro-grid concept. In addition, having an ESS could palliate the unmanageable nature of these sources of energy, allowing the set of PVGS and ESS to generate a constant power, eliminating or diminishing the fluctuations in the power generated by the PVGS.

Currently the feasibility of micro-grid is being analyzed, which could be managed as islands (or management areas that attempt to balance generation and consumption). These micro-grid would be interconnected, and would have generation systems, mainly from renewable sources (wind, photovoltaic,...) with the corresponding ESS. These ESSs could be made with different technologies, such as batteries, inertia frills, supercapacitors, or superconducting magnets [1].

In the design of future PIS for PVGS, in a context of gradual increase in the percentage of generation by these plants, the ESS will be of great importance, mainly because of the need to manage and optimize the flow of energy from such sources. Recent studies consulted use systems with batteries, supercapacitors or a hybrid of both [5].

The principal ESS and the most relevant ESS technology characteristics are summarized in Table I [6].

Table 1: Energy storage technologies

Technology	Power	Energy density	Back-up time	Response time	Efficiency	Lifetime(years)
Pumped hydro	100 MW – 2 GW	400 MWh – 20 GWh	hours	12 minutes	70 - 80 %	50
CAES	110 MW – 290 MW	1.16 GWh - 3 GWh	hours	12 minutes	90 %	< 50
BESS	100 W – 100 MW	1 kWh - 200 MWh	hours	seconds	60 - 80 %	< 10
Flywheels	5 kW – 90 MW	5 kWh – 200 kWh	minutes	12 minutes	80 - 85 %	20
SMES	170 kW – 100 MW	110 Wh – 27 kWh	seconds	milliseconds	95%	30
Supercapacitors	< 1 MW	1 Wh- 1kWh	seconds	milliseconds	> 95%	> 10

2.1 CAES (Compressed Air Energy Storage)

CAES uses the peaks of energy generated by renewable energy plants to run a compressor that compresses the air into a hermetic underground reservoir or surface vessel/piping. The compressed air is used, combined with a variety of fuels in a combustion turbine to generate electric energy when demand is high. The energy storage capacity depends on deposit volume and maximum storage pressure of the compressed air [6].

2.2 Pumped Hydroelectric

Pumped hydroelectric storage has been commonly used for 70 years. These plants are the most used for large scale applications at present [7].

2.3 Superconducting Magnets

A Superconducting Magnetic Energy Storage (SMES) system stores the energy as magnetic energy in a superconducting magnet cryogenically cooled, achieving a system with negligible losses. The AC energy is stored as DC energy and brought back from DC to AC energy from the superconducting magnet by a reversible AC/DC Power Converter Module (PCM).
The energy stored by an SMES is

$$E = \frac{1}{2} LI^2 \tag{1}$$

where L is the equivalent self-inductance of the superconductor system, and I is the DC current that flows through the winding. This current is the principal magnitude that the PCM uses for controlling the energy stored or generated by the system.

SMES efficiency is between 95 % and 98 %. It has a high availability, being able to supply high energy quantity in time intervals of milliseconds [9].

The main disadvantage of the SMES system is that the energy density is low and there is a need for a cryogenization system that could be very complex for large scale application. A possible solution is to combine them in hybrid ESS increasing their energy and power [10].

2.4 Flywheels

Due to their simplicity, flywheel energy storage systems (FESS) have been widely used in commercial small units (about 3 kWh) [10].

Energy is stored as kinetic energy using a rotor that rotates with high angular speed

$$E = \frac{1}{2} J\omega^2 \tag{2}$$

where J is the momentum of inertia and ω is the angular velocity.

The rotor is a hollow cylinder and has magnetic bearings to minimize friction. The rotor is located in a vacuum pipe to decrease its friction even more. The rotor is integrated into a motor/generator machine that allows the energy flow in both directions.

There are two topologies, slow flywheels (with angular velocity below 6,000 rpm) based on steel rotors, and fast flywheels (below 60,000 rpm) that use advanced material rotors (carbon fiber or glass fiber). FESS presents an efficiency of 80-85 %, with a useful life of 20 years.

The trend of FESS applied to the renewable energies is to combine them with other technologies, like micro CAES or thermal energy storage systems [11].

2.5 Batteries

These systems could be located in any place and be rapidly installed. Large systems (known as Battery Energy Storage System, BESS) don't have the environment impact of other ESS technologies and can be located in a building (or similar) near the point of demand

BESS uses a PCM to convert the battery DC energy into AC grid-compatible energy. These units present fast dynamics with response times near 20 milliseconds and efficiency from 60% to 80% [9].

The energy is stored as electro-chemical energy. The battery temperature change during charge and discharge cycles must be controlled because it affects its life expectancy.

Large scale BESSs that exist nowadays are the 10 MW (40 MWh) systems installed in China and California, and the 20 MW (5 MWh) system installed in Puerto Rico [9].

New battery technologies are being developed for a higher energy store capacity and at a lower cost than the Lead Acid battery. Some of these new technologies are Lithium Ion, Regenesys® Redox, Nickel Metal Hydride, Hydrogen Vanadium Redox, Nickel Cadmium and Zinc Bromide [12].

2.6 Supercapacitors (ultracapacitors)

The energy stored in supercapacitor Energy Storage System (SESS) will depend on the voltage at the ends, such as

$$E = \frac{1}{2} C V^2 \tag{3}$$

where V is the supercapacitor voltage.

The specific capacitance of such a double-layer is given by

$$C = \varepsilon_0 \varepsilon_r \frac{A}{D} \tag{4}$$

where C is the capacitance, ε_0 the dielectric constant of free space, ε_r the dielectric constant of the medium between the two layers, A the surface area, and D is the distance between the two layers (the distance from the electrode surface to the center of the ion layer). This approximation is roughly correct for concentrated electrolytic solutions.

The most relevant properties of the SC, compared to conventional capacitors, are its high capacity values (approximately thousands of Farads), greater energy density (10 Wh/kg), and power (50 kW/kg), a high efficiency (above 95 %) and low maintenance cost and longer life [13]-[19].

In this paper considers that the ESS is built from SC. The SC is an emerging technology that is beginning to be applied for the implementation of ESS for PVGS. These devices can be implanted easily in existing systems of power injection because their behavior is similar to a conventional capacitor.

SESS voltage must be limited to a maximum value, V_{max}, so also there is a limit to the maximum amount of energy, W_{max}, which can be stored in the SC.

Similarly it is desirable to limit the minimum voltage of the SESS, V_{min}, to ensure that the converter responsible for the SESS control works in a proper operating range. Defining an index of change in voltage, Δ, as the ratio between V_{min} and V_{max}, expressed as a percentage, it is possible to obtain the energy available (when the SESS is charged) as:

$$W_{SESS} = \frac{N}{2} C V_{max}^2 \left(1 - \left(\frac{\Delta}{100}\right)^2\right), \tag{5}$$

where N is the number of SC modules in series that the SESS contains. From the above equation it is possible to deduce the number of SC that are needed to build the SESS.

3 Energy storage capacity

As mentioned above, the idea is to design a system that transforms renewable energy in quasi-manageable, and for this purpose a SESS has been designed, assuming that the set PVGS-SESS behaves as a conventional power source delivering the power which is demanded.

The design of the SESS done assumes that the set PVGS-SESS must behaves as a constant power source for pre-established time intervals. For this analysis is considered a PVGS with nominal peak power equal to 100 kWp. The result can be easily extrapolated to other PVGS powers. As it is well known the power generated by a PVGS in a regular weather conditions depend on the time of day as shown in Fig 3.

When determining the interval of constant injected power into the grid, it has been considered the symmetry of the generated power for optimizing the variations of storage energy.

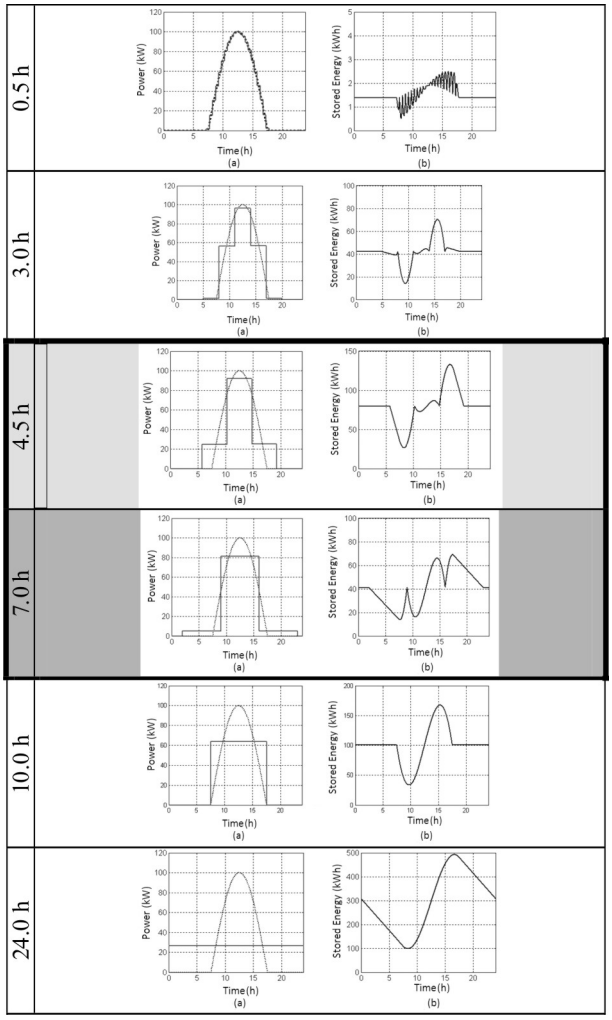

Figure 3: Power and energy for different constant injected power interval lengths: a) Generated and injected power; b) energy stored in the SESS.

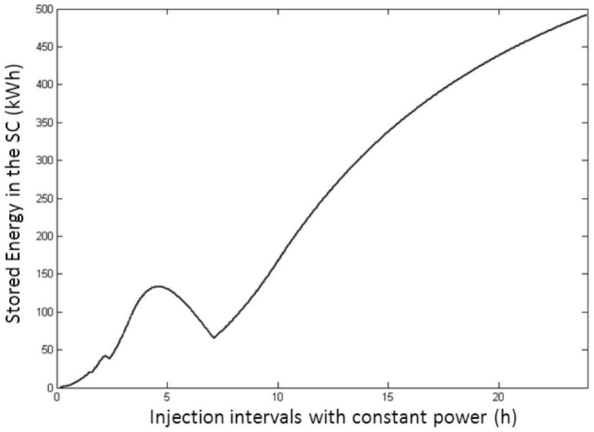

Figure 4: SESS Capacity versus the length of constant injected power intervals.

Also, it has been taken into account that the minimum storage energy must be at least 20% of the maximum energy for guarantying a minimum voltage that allows the control electronics to operate correctly, as the DC / DC converter present buck/boost margin.

The variation of the SESS storage capacity when varying the length of the constant injected power interval is shown in Fig. 4. It is highlighted that for an interval length of 3 and 7 hours is needed the same storage capacity, being better the 7 hours interval that ensures constant injected power during more time. It is also highlighted that the constant injected power interval length equal to 4,5 hours produces a relative maximum being worse that the 7 hours option.

4 Description of the proposed system

The proposed scheme for the PVGS connected to the grid, is shown in Fig. 5. The inverter used is of high switching frequency (10-20 kHz). The SESS control is performed using a bidirectional DC/DC converter.

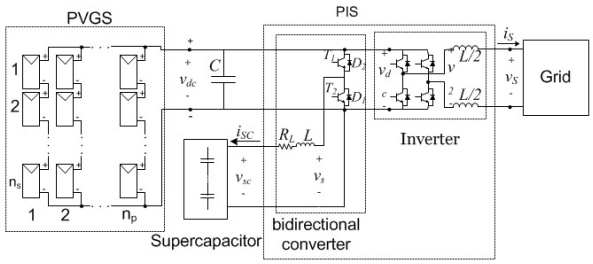

Figure 5: Proposed system scheme.

The main objective of the proposed system is to inject a constant power into the grid following a reference value, charging or discharging the SESS depending on the power generated by the PVGS being higher or lower than the reference power. The control electronic system is conformed by two converters: the inverter and a bidirectional DC-DC converter.

4.1 Inverter

The inverter's purpose is to inject the energy generated by the PVGS into the grid, producing sinusoidal currents in phase with the voltages. To control the active power that is injected, it is sufficient, if the voltage is perfectly sinusoidal, to control the fundamental component of the stress of the inverter. The MPPT routines are also developed by the inverter.

As mentioned, the inverter controls the current injected into the grid using a synchronous hysteresis band [1], [18] with a switching frequency of 20 kHz. The inverter must build the power supply with the desired quality.

4.2 BiDDC: Bidirectional DC/DC converter

To control the SESS a BiDDC has been chosen, which allows a correct operation of the system opposite the changes in SC terminals due to variations in the energy stored in them, also allowing bidirectional power flow and hence the charging and discharging of the SESS.

The converter has three operating modes: a first charging mode, in which the energy flow is from the PVGS towards the SESS (which will occur when the power generated by the PVGS is greater than the reference operation point or when the SESS voltage is less than the start-up voltage); a second mode, of discharge, where the energy will flow from the SESS to the grid (via the inverter, which will occur when the power generated by the PVGS is less than the power reference operation point); and a third mode, stand-by, where there is no flow of energy (which occurs when the power generated by the PVGS is lower than the set point and the voltage of the SESS in lower than the one of start-up).

4.2.1 Charge mode

In this mode of operation, the energy goes from the PVGS (through the DC bus) towards the SESS, making the control through the switching of T_2.

By closing the switch T_2 the current passes through the L_{SC} towards the SC (Fig. 6a). In that time interval, some energy is dissipated in R_L, some accumulates in L_{SC} (increasing the current), and the rest, the largest amount, is stored in the SESS. The free movement diode D_1 conducts when the switch T_2 is closed and the current goes out from the SC (Fig. 6c).

In the steady state, considering that there are no losses, the increase in i_L during closing of the switch must be equal to the decrease when the switch is opened. The input power must be the same as the converter output power. Because of this, we find that the work cycle of the switch T_2 satisfies the following relation:

$$D_2 = \frac{T_{on,T_2}}{T} = \frac{V_{SC}}{V_{dc}} = \frac{I_{dc}}{I_{SC}}. \tag{6}$$

This index represents the percentage of time T_2 remains closed during each switching cycle.

In this mode of operation, the converter behaves like a DC transformer (transformation ratio, a = D_2) and to make it work we must have $D_2 \geq V_{SC} / V_{dc}$.

The ripple of the SESS current is calculated from the positive slope that occurs when the switch T_2 is closed, neglecting the resistance of the coil R_L:

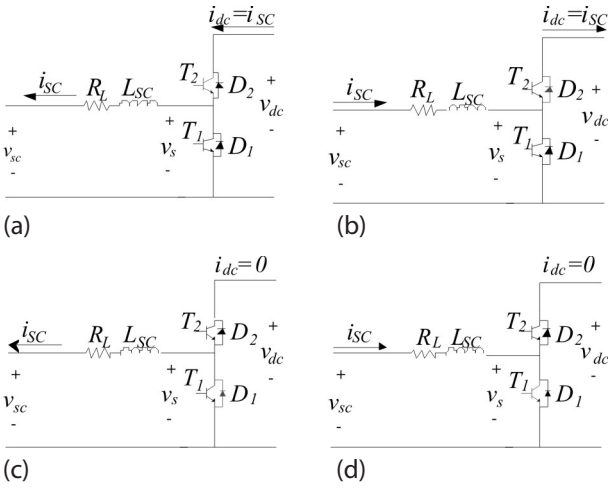

Figure 6: BiDDC Operation modes: a) Charge mode with power flow; b) Discharge mode with power flow; c) Charge mode without power flow d) Discharge mode without power flow

$$\Delta i = \frac{V_{dc}}{L_{SC} f} D_2 \left(1 - D_2\right), \tag{7}$$

where f is the switching frequency. A small ripple is desirable, and the maximum ripple occurs for $D_2 = 0.5$. and when the voltage $V_{SC} < V_{dc} / 2$. The design variables to control this ripple are the switching frequency, f, and inductance value, L_{SC}.

To control the transfer of energy, the flow of the SESS is controlled with a synchronous hysteresis band controller, which controls the voltage applied to the coil terminal.

If the applied voltage is lower than V_{SC}, there will be no current flow because it cannot pass through the diode D_1 (reverse direction), or through T_1 (switched off). If the modulated voltage is greater than V_{SC}, the current averaged over one switching period depends on the resistance R_L. The following expression sets the value

$$\overline{I_L} = \frac{V_{dc} D_2 - V_{SC}}{R_L}. \tag{8}$$

From this equation we deduce that for the existence of an energy transfer to V_{SC}, we need a modulation index D_2 greater than V_{SC} / V_{dc}.

4.2.2 Discharge mode

In this mode of operation, the energy goes from the SESS to the grid (through the DC bus and the inverter). In this mode the control is performed by the switching of T_1.

This mode of operation increases the current in the coil L_{SC} when the switch T_1 is closed (Fig. 6d). if the current goes in the opposite way (Fig. 6b) the current through L_{SC} decreases and passes through the diode D_2 towards the DC bus.

As the previous operation mode, the current flow through the SESS is controlled through the voltage applied in the coil L_{SC} terminal.

The current i_L increment when the switch is closed must be equal to its decrement when the switch is opened. And considering that there are no losses, the input power must be the same as the converter output. We reach the transformation ratio:

$$\frac{1}{1-D_1}=\frac{V_{dc}}{V_{SC}}=\frac{I_{SC}}{I_{dc}}. \tag{9}$$

Modulation index D_1 represents the percentage of time T_1 remains closed during each switching cycle.

In this mode of operation, the converter behaves like a DC transformer (with a transformation ratio of a = 1/(1-D_1)) and works as long as (1-D_1) ≥ V_{SC}/ V_{dc}.

Operating the same way as in the previous case, we can calculate the value of current in the DC bus

$$\overline{I_L}=\left(\frac{V_{SC}}{1-D_1}-V_{dc}\right)\Big/\left(\frac{R_L}{(1-D_1)^2}\right). \tag{10}$$

Actually, T_1 is triggered in a complementary way with respect to T_2, so it is possible to define one duty cycle $D=D_2=1-D_1$.

5 Control system

The control can be divided into blocks which are shown in the diagram represented in Fig. 7.

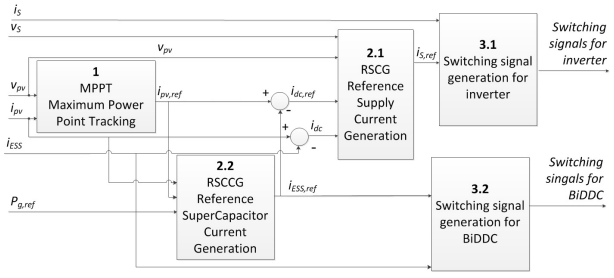

Figure 7: PVGS system control squeme.

The Maximum Power Point Tracking, Reference Supply Current Generation and Generation of switching signals to inverters blocks are implemented as described in [20].

This block generates the inverter switching signals using a synchronous hysteresis band that compares with zero, in each sampling period, the error existing between the reference supply current and the measured supply current [20].

The switching signals of the DC/DC bidirectional converter are generated by a synchronous hysteresis band that compares with zero, in each sampling period, the error existing between the reference current of the SESS and the measured current of the SESS.

The SESS reference current is obtained as the current that we would have to inject into the SESS to cancel the difference existing between the reference power that has to be injected into the grid and the actual power generated by the PVGS.

6 Simulation Results

The simulations are done in two steps. Firstly, the energy storage system based on supercapacitors is analyzed in electrical terms by maintaining a constant irradiance. Secondly, the behavior of the system is exposed when there are irradiance fluctuations.

Fig. 8 shows the scheme of the simulated system, which simulates a PIS, capable of establishing and maintaining the PVGS in its MPP and injecting the value of the power established. The PVGS model used in the simulation offers the properties exposed in [21]-[22]. The main features of PVGS and PIS are shown on Tables II and III. The power converter model was developed by using switching states. The simulated PVGS has 16 photovoltaic cells connected in series (Shell SP-150-P), which maximum power point voltage is 544 V for nominal conditions of irradiance of 1000W/m^2 and temperature of 25ºC.

Table 2: PVGS Characteristics

Parameter	Value
Number of series-parallel connected cells	16-1
Photovoltaic cell reference	SHELL SP150-P
Short-circuit current (25ºC, 1000W/m2)	4.8 A
Open-circuit voltage (25ºC, 1000W/m2)	43.4 V
MPP current (25ºC, 1000W/m2)	4.4 A
MPP voltage (25ºC, 1000W/m2)	34 V

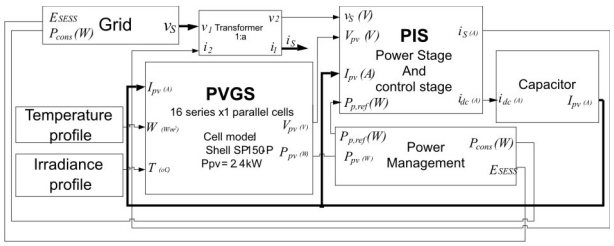

Figure 8: Simulated System scheme.

Table 3: PIS parameters for simulations

Parameter	Valor	Parameter	Valor
Inductance L	2x50 mH	Capacitor C	64.36 µF*2
Inductance L_C	100 mH	Inductor resistance R_L	0.01 Ω
Switching frequency			20 kHz

Through the analysis of power reference profile shown in Fig. 9, the evolution of the power of a stand-alone SESS is observed (Fig.º10). SESS consists of 6 modules in series with a capacity of 1.65 F, 100 times less capacity than the commercial module of reference BMOD165P048 from Maxwell Technologies, to reduce the duration of the simulations. The control of the system avoids that the SESS is completely uncharged, turning off by its-self when the SESS voltage catches a minimum value. In Fig. 10 one can check the stand-alone SESS control dynamic performance. As the power is directly proportional to the voltage and the flow, for the power to be constant, when the voltage in SESS rises, the flow has to go down and vice versa. In other words, as we can appreciate in Fig 10 and 11, when the SESS is loaded the system requires less flow to maintain the same power.

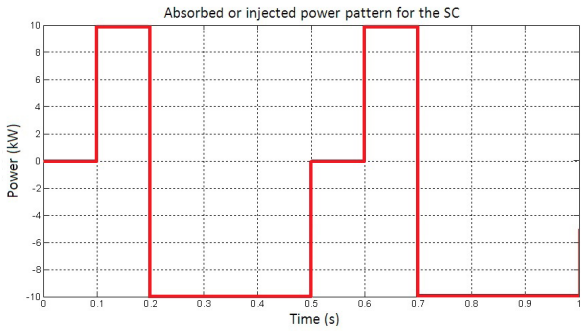

Figure 9: SESS power pattern.

Finally, a simulation of the complete system shown in Fig. 8 is carried out for the irradiance profile shown in Fig. 12. This irradiance profile has been selected to evaluate the behavior of the entire system (including the SESS) when varying conditions occur. In Fig. 13 we observe that the system fulfills the specifications of

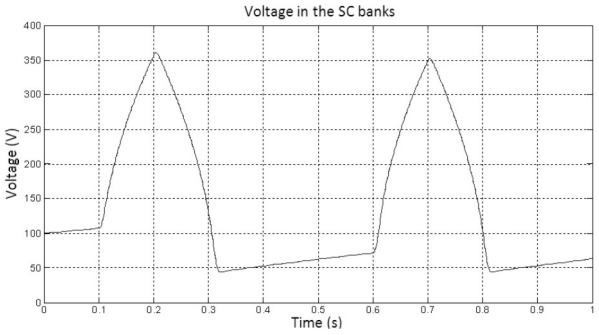

Figure 10: SESS voltage.

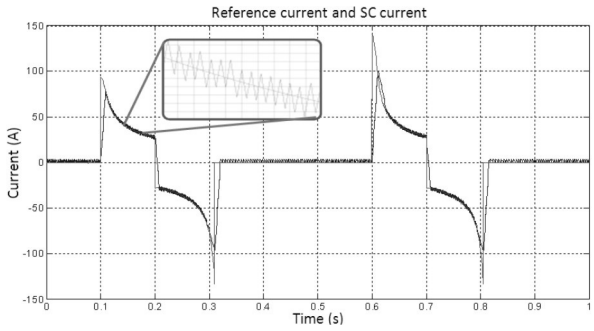

Figure 11: Reference current and SESS current.

not injecting power in the grid until the SESS obtains a minimum voltage. Once it has obtained this voltage the SESS is capable of absorbing and injecting energy and controlling the power injected in the grid. At this point, the system begins to inject the constant power (or set point) even though there are variations in the irradiance.

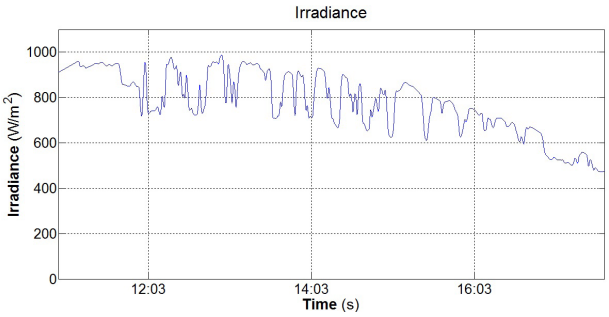

Figure 12: Irradiance profile for simulation test.

Fig. 14 and 15 show respectively the flow and the voltage of the SESS. Fig. 16 shows a detail of the flow injected in the grid by the inverter that is in phase with the voltage. As it can be seen, the system maintains the power reference despite of the irradiance changes.

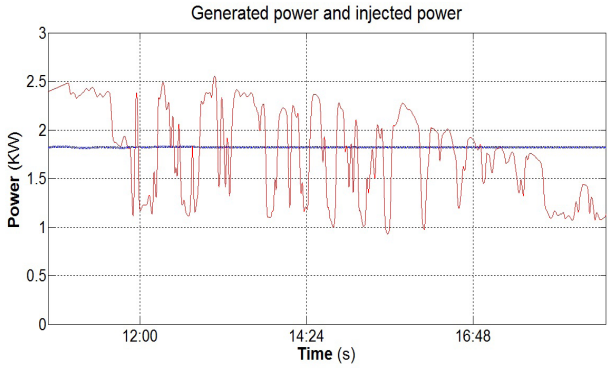

Figure 13: PVGS generated power and power injected to the grid.

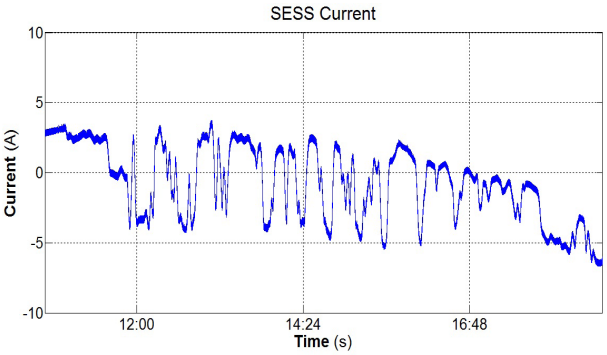

Figure 14: SESS current.

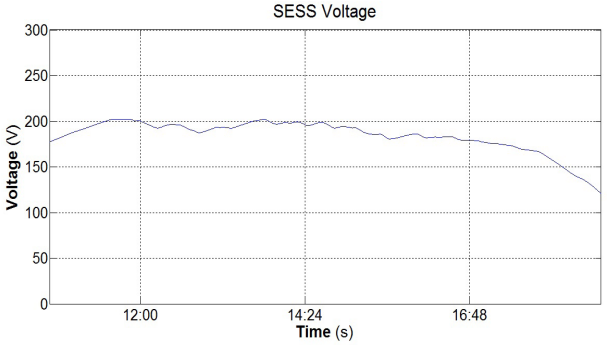

Figure 15: SESS voltage.

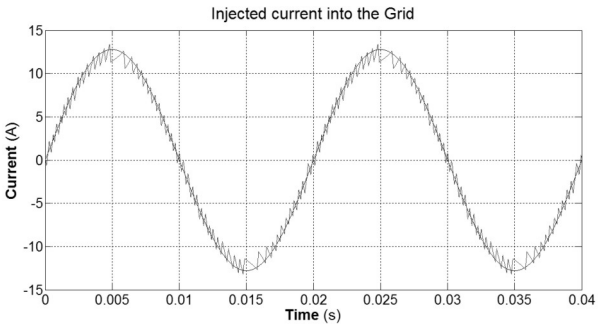

Figure 16:. Current injected to the grid.

7 Experimental results

The PVGS-SESS prototype has been tested experimentally, Fig 17, to verify its correct functioning. This prototype is composed of an electronic converter SEMITRANS Stack with four SKM50GB123D SEMIKRON branches, three for the VSI and one for the DC / DC converter, four SKHI 22 drivers and a Maxwell Technologies supercapacitor BMOD0165 P048 B01. To model the photovoltaic plant a solar array simulator HP E4351B has been used.

The control platform used is a control board NI sbRIO9632 FPGA/Processor with the Development software LabVIEW 2011 SP1. The measurements were made with Voltage transducers LV 55-P and Current transducers LA 55P/SP1.

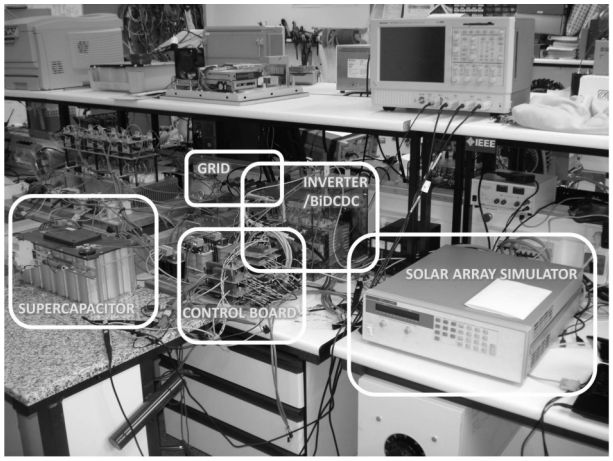

Figure 17: Experimental prototype.

is 20 kHz. The PLL is implemented here in order to maintain the synchronization with the grid despite of voltage distortions or grid events. And the PI controller is also implemented in the FPGA together with the SC and grid current references with the purpose of providing a fast response.

The processor is taken for the slower tasks, such as MPPT, and the high computational cost tasks, such as power calculations. It is synchronized with the FPGA with the Scan Engine feature at 10 ms and the sample rate of the loop is 200 ms.

Some experimental tests have been carried out to validate the control system and the prototype performance. Fig 18 shows the waveforms when the system is working in the steady state during the process of loading and unloading the SESS.

Fig 19 (a) shows the transient state of the PVGS-SESS system when it operates without the SESS. In this case

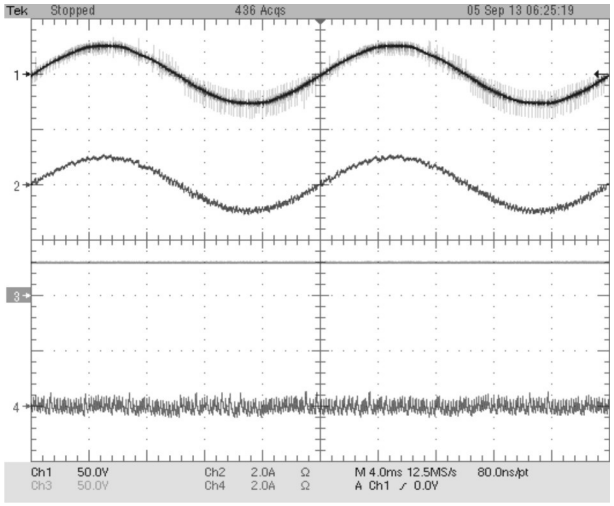

a.

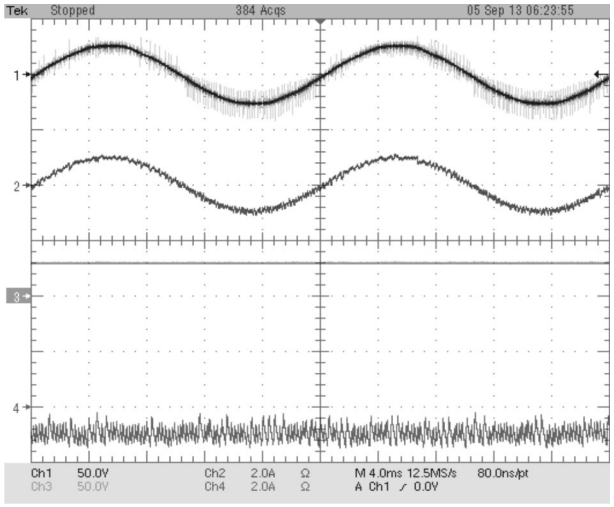

b.

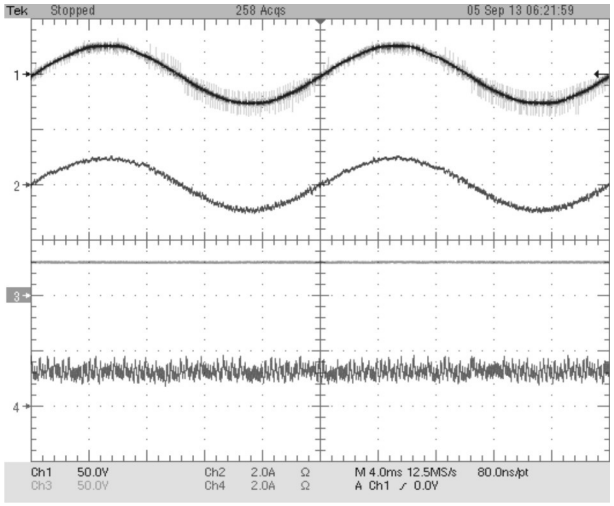

c.

Figure 18: Steady state experimental waveforms: (a) Injecting the same power than the PV panels, (b) Injecting less power than the PV panels, and (c) Injecting more power than the PV panels energy.

the aim is to inject the maximum power available from the PV system. To obtain this, the current is injected in phase with the voltage, so that voltage and current of the same phase are synchronized. In Fig. 19 (a) one can see how the injected power reaches the MPP and stabilizes with active power control disabled. The test also adds a disconnection and the start procedure again.

However, when you activate the SESS, the active power injected is the one demanded by the grid manager. Following the same pattern, when the SESS is enabled, Fig 19(b) shows how the power injected into the grid matches the reference. This is because the DC / DC converter is the one that injects the energy required until the MPP is achieved. It is easy to see how the active power injection instantly becomes the reference thanks to the SESS, so the MPPT setup procedure does not matter.

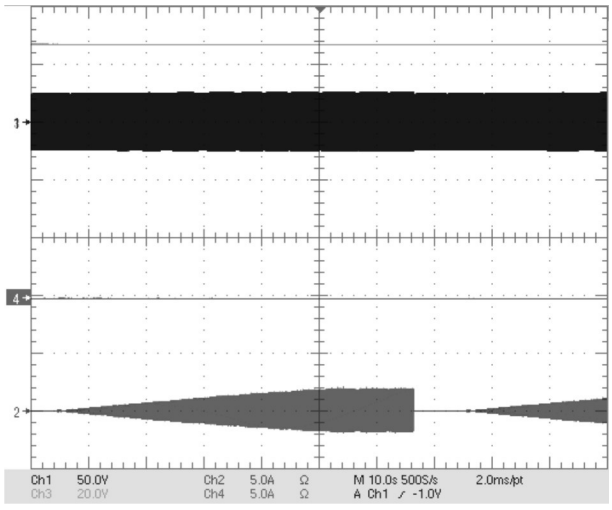

a.

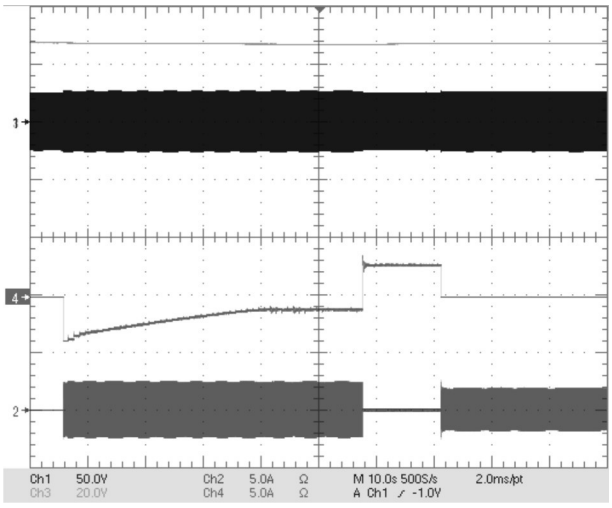

b.

Figure 19: Transient state experimental waveforms: (a) Injecting without active power control, (b) Injecting with different active power references.

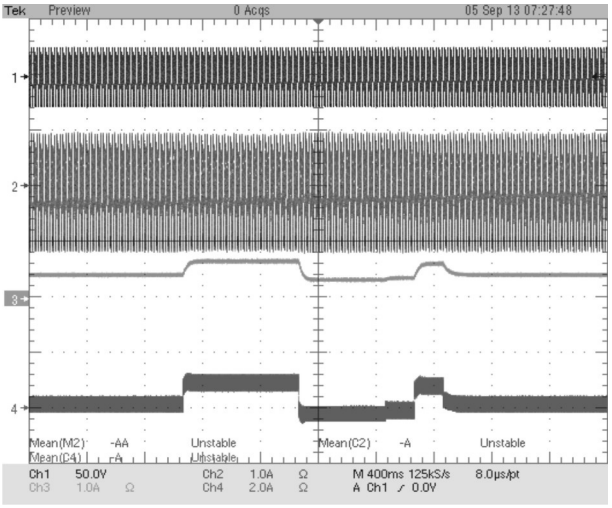

a.

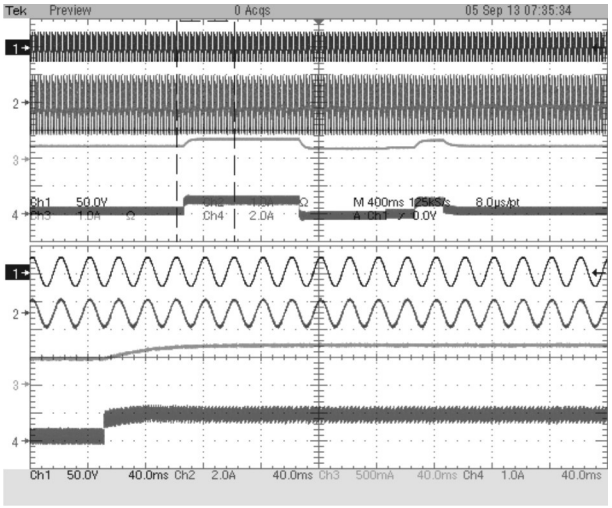

b.

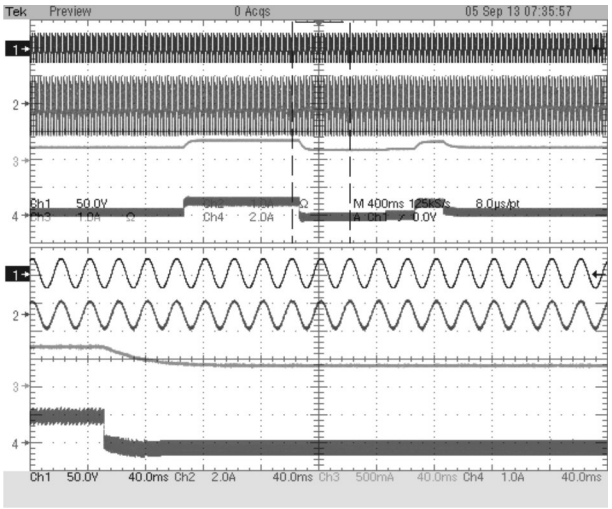

c.

Figure 20: Transient state experimental waveforms: (a) Injecting with different value of active power generation, (b) and (c) Details of the dynamics of the system.

Figure 20 shows the evolution of the PVGS-SESS system when the irradiance changes. The irradiance profiles are introduced by interfacing the solar array simulator. As it can be seen in Fig 20 (a), these changes of irradiance cause fluctuations in the power generated by the PV that also are observed in PV current, and the PVGS-SESS system reacts storing or supplying energy in the SC.

In Fig 20 (b) and Fig 20 (c) the dynamic response of the system can be seen. In this situation, the system, due to an excess or a shortage of energy generated, reacts and is able to inject the set reference power. This is because of the DC / DC converter injects the energy required until the reference power is obtained. As mentioned above, the active power injection instantly becomes the reference thanks to the SESS.

8 Conclusion

In this paper a new topology for the power injection system used in photovoltaic generation systems is presented. This topology is based on two converters, a voltage source inverter that injects the power into the grid and a bidirectional direct current converter that regulates the charge of the SC. The performance of the proposed system was tested by simulation and by a laboratory prototype. The proposed system dampens the fluctuations and maintains the reference power injected into the grid by the PVGS during the time set by the grid manager, showing the benefits of using a SESS in an injection system connected to the grid for photovoltaic generators. On the one hand, the MPPT transients do not affect to the desired injected power, and on the other hand, the irradiance changes maintain the injected power reference. Its operation is based on the traditional energy generation, making renewable energy generation "quasi-manageable".

It is easy to incorporate a SESS into the existing inverter topologies, being able to maintain constant the power injected into the grid, having a good steady and transient state performance. The time interval which ensures the power injected determines the size or capacity of the SESS. It is important to note how higher intervals need the same capacity than smaller ones, due to the symmetry over the time of the day of the generated power, but longer intervals guarantee a better integration into the distribution grid management. Finally, we showed how the PVGS can be improved, in order to ensure maximum energy extraction and guarantee that the set reference power is delivered.

9 Acknowledgement

This work has been supported by the Government of Extremadura (Spain) and the European Regional Development Fund (research project PCJ1004).

10 References

1. J. M. Carrasco, L. G. Franquelo, J. T. Bialasiewicz, E. Galvan, R. C. Portillo Guisado, M. A. M. Prats, J. I. Leon, and N. Moreno-Alfonso, " Power-electronic systems for the Grid integration of renewable energy sources: A survey," IEEE Trans Ind. Electron., vol. 53, nº. 4, pp. 1002–1016, June 2006.
2. Kern, E.C., Jr.; Gulachenski, E.M.; Kern, G.A.," Cloud effects on distributed photovoltaic generation: slow transients at the Gardner, Massachusetts photovoltaic experiment"IEEE Transaction on Energy Conversion, vol. 4, Issue 2, Page(s):184 - 190, June 1989
3. A. Woyte, Vu Van Thong, R. Belmans, J. Nijs, "Voltage Fluctuations on Distribution Level Introduced by photovoltaic Systems", IEEE Transactions on Energy Conversion, Vol. 21, nº 1, March 2006.
4. Jurij Kurnik, Marko Jankovec, Kristijan Brecl, Marko Topič, " Development of outdoor photovoltaic module monitoring system". Informacije MIDEM 38 (2008) 2, pp. 75-80.
5. Jinhui Xue, Zhongdong Yin, Bingbing Wu, Ziping Wu, Jun Li,"Technology Research of Novel Energy Storage Control for the PV Generation System", IEEE Conference on Power and Energy Engineering, Page(s):1 - 4, March 2009.
6. Smith, S.C.; Sen, P.K.; Kroposki, B., "Advancement of energy storage devices and applications in electrical power system," Power and Energy Society General Meeting - Conversion and Delivery of Electrical Energy in the 21st Century, 2008 IEEE , vol., no., pp.1,8, 20-24 July 2008.
7. H. Ibrahim, A.Ilinca, R.Younès, J.Perron, T.Basbous, "Study of a Hybrid Wind-Diesel System with Compressed Air Energy Storage", IEEE Conference on Canada Electrical Power, Page(s):320-325, October 2007.
8. W. Leonard, and M. Grobe, "Sustainable Electrical Energy Supply with Wind and Pumped Storage–A Realistic Long-Term Strategy or Utopia", IEEE General Meeting of Power Engineering Society, pp. 1221-1225, June 2004.
9. Derk J. Swider, "Compressed Air Energy Storage in an Electricity System with Significant Wind Power Generation", IEEE Transactions on Energy Conversion, vol. 22, no. 1, pp. 95-102, March 2007.
10. Robert B. Schainker, "Executive Overview: Energy Storage Options For A Sustainable Energy Future", IEEE Power Engineering Society General Meeting, Page(s):2309-2314, vol. 2, June 2004.
11. Toshifumi Ise, Masanori Kita, and Akira Taguchi,"A Hybrid Eenrgy Storage with a SMES and Secondary Battery", IEEE Transactions on Applied Superconductivity, vol. 15, No. 2, June 2005.
12. J. R. Sears, "TEX: The next generation of energy storage technology", in Proc. 26thAnnu. Int. Telecommun. Energy Conf., Sep. 2004,pp.218–222.
13. John P. Barton and David G. Infield, "Energy Storage and Its Use With Intermittent Renewable Energy", IEEE Transactions on Energy Conversion, vol. 19, No. 2, pp.441-448, June 2004.
14. A. Burke, "Ultracapacitors: Why, how, and where is the technology", J. Power Sources, vol. 91, pp. 37-50, 2000
15. Y. Y. Yao, D. L. Zhang, and D. G. Xu, "A Study of Supercapacitor Parameters and Characteristics", IEEE Conference on Power System Technology, Page(s):1 - 4, October 2006
16. Tongzhen Wei, Sibo Wang, Zhiping Qi, "A Supercapacitor Based Ride-Througth System for Industrial Drive Applications", IEEE Conference on Mechatronics and Automation, Page(s):3833 - 3837, August 2007
17. G. Alcicek, H. Gualous, P. Venet, R. Gallay, A. Miraoui, "Experimental study of temperatura effect on ultracaapcitor ageing", IEEE Conference on Power Electronics and Applications, Pages(s):1-7, September 2007.
18. A. B. Cultura II, and Z. M. Salameh, "Performace Evaluation of a Supercapacitor Module for Energy Storage Applications", IEEE Power and Energy Society General Meeting, Page(s):1-7, July 2008
19. W. Jewell, R. Ramakumar,"The Effects of Moving Clouds on Electric Utilities with Dispersed Photovoltaic Generation",IEEE Transactions on Energy Conversion, Vol. EC-2, pp 570 - 576 December 1987.
20. A. B. Cultura II, and Z. M. Salameh, "Performace Evaluation of a Supercapacitor Module for Energy Storage Applications", IEEE Power and Energy Society General Meeting, Page(s):1-7, July 2008
21. E. Romero-Cadaval,M.I. Milanés-Montero, E. González-Romera, F. Barrero-González, "Power Injection System for Grid-Connected Photovoltaic Generation Systems Base don Two Collaborative Voltage Source Inverters" IEEE Transactions on Industrial Electronics. Vol. 56, no. 11, pp. 4389-4398, 2009.
22. Carlos Roncero Clemente, Oleksandr Husev, Víctor Miñambres Marcos, Serhii Stepenko, E. Romero-Cadaval, Dmitri Vinnikov "Comparison of Three

MPPT Algorithms for Three-Level Neutral-Point-Clamped qZ-Source Inverter". Compatibility and Power Electronics, 2013. CPE '13, pages 80 – 85. June 2013.
23. Jože Rakovec, "Exploiting solar energy with photovoltaics". Informacije MIDEM 39 (2009) 4, pp. 213-215.

Arrived: 13. 09. 2013
Accepted: 15. 01. 2014